Effects of Hydrostatic Pressure on the Thermodynamics of CspB-Bs Interactions with the ssDNA Template

Samvel Avagyan[a,c] and George I. Makhatadze[a,b,c*]

[a] *Department of Biological Sciences, Rensselaer Polytechnic Institute, Troy, NY 12180, USA*
[b] *Department on Chemistry and Chemical Biology, Rensselaer Polytechnic Institute, Troy, NY 12180, USA*
[c] *Center for Biotechnology and Interdisciplinary Studies, Rensselaer Polytechnic Institute, Troy, NY 12180, USA*

*Corresponding Author: George Makhatadze, Center for Biotechnology and Interdisciplinary Studies, Rensselaer Polytechnic Institute, Troy, NY 12180, USA makhag@rpi.edu

Keywords: Protein-DNA interactions; thermodynamics; high hydrostatic pressure; osmolytes; Cold shock proteins

ABSTRACT

Understanding the thermodynamic mechanisms of adaptation of biomacromolecules to high hydrostatic pressure can help shed light on how piezophilic organisms can survive at pressures reaching over 1000 atmospheres. Interactions of proteins with nucleic acids is one of the central processes which allows information flow encoded in the sequence of DNA. Here we report the results of a study on the interaction of cold shock protein B from *Bacillus subtilis* (CspB-BS) with heptadeoxythymine template (pDT7) as a function of temperature and hydrostatic pressure. Experimental data collected at different CspB-Bs:pDT7 ratios were analyzed using a thermodynamic linkage model, that accounts for both protein unfolding and CspB-Bs:pDT7 binding. The global fit to the model provided estimates of the stability of CspB-Bs, ΔG^o_{Prot}, the volume change upon CspB-Bs unfolding, ΔV_{Prot}, the association constant for CspB-Bs:pDT7 complex, K^o_a, and the volume changes upon pDT7 ssDNA template binding, ΔV_{Bind}. The protein, CspB-Bs, unfolds with increase in hydrostatic pressure (ΔV_{Prot} <0). Surprisingly, our study showed that ΔV_{Bind}<0, which means that the binding of CspB-Bs to ssDNA is stabilized by increase in hydrostatic pressure. Thus, CspB-Bs binding to pDT7 represents a case of linked equilibrium in which folding and binding react differently upon increase in hydrostatic pressure: protein folding/unfolding equilibrium favors the unfolded state, while protein-ligand binding equilibrium favors the bound state. These opposing effects set a "maximum attainable" pressure-tolerance to the protein-ssDNA complex under given conditions.

INTRODUCTION

Life has adapted to strive in many different conditions, both on land and sea. One such condition is high hydrostatic pressure. In the deep oceans and subsurface of the crust, high pressure is the universal stressor to which all life forms must adapt. This is because hydrostatic pressure affects the macromolecular equilibrium of biomolecules. Thermodynamically, the pressure (P) dependence of equilibrium constant (K_{eq}, and thus the Gibbs energy, ΔG) in a two-state system is defined by the volume changes (ΔV_{Tot}) as:

$$-RT\left(\frac{\partial \ln(K_{eq})}{\partial P}\right)_T = \left(\frac{\partial \Delta G}{\partial P}\right)_T = \Delta V_{Tot} = (V_{State2} - V_{State1}) \quad 1.$$

Thus, according to the Le Chatelier principle, if ΔV_{Tot} is negative increase in pressure will shift equilibrium to State1, while if ΔV_{Tot} is positive, the equilibrium will be shift to State2.

It is known that hydrostatic pressure can change the equilibrium between native (N) and unfolded (U) states of a protein, $\Delta V_{Prot} = (V_U - V_N)$. Experimental and computational analysis of volume changes upon unfolding have shown that ΔV_{Prot} for the majority of proteins is negative, although some proteins have been reported to have small but positive ΔV_{Prot} values [1]. In our previous work we explored the idea that organisms adapted to high pressure environments will have acquired adaptations in the protein sequences that make the proteins more pressure-stable than proteins fom their non-piezophilic counterparts [2]. We applied a computational method to predict volume changes upon protein unfolding [1, 3] to proteomes of piezophilic and non-piezophilic organisms. This was done to test the hypothesis that the proteins of piezophiles will undergo volume changes that are less negative or even positive, when compared to the proteins of non-piezophiles. Our study indicated that pressure-stability among piezophilic and non-piezophilic proteomes are comparable. This suggested to us that modulating the ΔV_{Prot} of their proteomes is not a mechanism that organisms have employed in order to counteract the denaturing effects of high pressure. While the ΔV_{Prot} may not be under evolutionary pressure for stabilizing protein monomers against high pressures, the question of what molecular mechanisms that piezophiles adopt to counteract the effects of high pressures still remains.

Previously, it has been shown that multimeric proteins, and protein macromolecule complexes are especially sensitive to high pressure. For example, this can be observed as inhibition of DNA replication, or RNA synthesis, alterations in gene expression patterns, inhibition of protein synthesis, depolymerization of previously polymeric proteins, to name a few [4-8]. In fact, these pressure-induced changes occur at much lower pressures than unfolding of monomeric proteins [9]. Furthermore, the pressure-induced injuries of non-piezophilic organisms occurs at pressures that are easily tolerated by piezophilic ones [9]. This suggests that piezophilic organisms may have acquired adaptations which stabilize their protein-ligand complexes from pressure dissociation. From the perspective of thermodynamic mechanisms, ligand-binding proteins from piezophilic and non-piezophilic organisms may exhibit unique binding volumetric properties ($\Delta V_{Bind} = V_{Protein/Ligand} - (V_{Protein} + V_{Ligand})$ which when compared to each other may elucidate a unique mechanism for adaptation to high pressures [10-11]. Such differences may be observed if the total volume of a bound state is larger than the unbound state, thus at high pressures the equilibrium binding reaction will shift to the unbound state, destabilizing the bound complex. However, if the total volume of the bound state is smaller than the unbound state, than at high pressure the equilibrium reaction will shift towards the bound state and this will act to further stabilize the binding.

As a first step in elucidating the effects of hydrostatic pressure on protein-ligand interactions, we studied the binding of cold shock protein B from *Bacillus subtilis* (CspB-Bs) to the single stranded heptadeoxythymine (pDT7). CspB is a biophysically tractable model system due to its high solubility, availability of structural information, and well-characterized nucleic acid binding affinity and specificity [12-16]. Most importantly, CspB also belongs to the Oligonucleotide/Oligosaccharide Binding fold (OB-Fold) that is found in all domains of life[17] and this feature will be important for future comparative studies of Csp proteins from other organisms.

Here we report a detailed experimental characterization of CspB-Bs binding to pDT7 ssDNA template as a function of temperature and pressure. Comprehensive analysis of the data using a thermodynamic linkage model reveals a number of interesting features. Most notably, the binding CspB-Bs binding to pDT7 ssDNA template is accompanied by negative volume changes, suggesting that increase in hydrostatic pressure actually stabilizes CspB-Bs: pDT7b complex. Additional experimental validation of this is provided by performing experiments is solution with stabilizing osmolyte, glutamate. The possible functional relevance of these findings for piezophilic adaptation is discussed.

METHODS

Protein Expression and Purification

CspB-Bs (UniProtKB - P32081) was expressed using *E. coli* BL21(DE3) containing the pCSP3 plasmid. The plasmid contained a CspB-Bs gene under T7 RNA polymerase control. The purification protocol for CspB-Bs was adapted from Lopez et. al. with modifications [13]. Cells were grown at 37°C in Fernbach flasks containing 1 L 2xYT media supplemented with 100 µg/mL ampicillin. The optical density of the cultures was monitored at 600 nm until they reached ~0.6 o.u.. Isopropyl-β -D-thiogalactopyranoside (IPTG) was added to a final concentration of 1 mM to induce protein production for five hours. Bacterial culture was harvested by centrifuging the culture at 7,500 x g. The pellets were frozen dry at -20°C until further processing.

Pellets were thawed and resuspended in 20 mM Tris, pH 7.5, 1 mM EDTA and passed through a French Press twice. The cell lysates were collected and centrifuged at 40,000 x g for one hour to remove insoluble cellular debris. The CspB-Bs was purified by first performing an ammonium sulfate precipitation. Ammonium sulfate to 40% saturation at 4°C was added to the clarified lysates and allowed to stir for at least 3 hours. The formed precipitate was removed by centrifugation at 7,500 x g. Ammonium sulfate to 90% saturation at 4°C was added to the supernatant and allowed to stir overnight. The formed precipitate was removed by centrifugation at 7,500 x g. The precipitate was collected, dissolved in water, and dialyzed (using 3 kD cutoff tubing) against water containing ~0.13% ammonium hydroxide v/v. The dialyzed solution was collected from the dialysis tubing and lyophilized. The lyophilized powder was dissolved in 20 mM Tris, pH 7.5, 1 mM EDTA. The protein solution was bound to a Fast Flow Q-Sepharose anion exchange column that was pre-equilibrated with the same buffer. After binding, the column was washed with 5 column volumes of buffer. The protein was eluted with a linear 0-500 mM NaCl gradient. Protein containing fractions were collected, dialyzed against water containing ~0.13% ammonium hydroxide v/v, and lyophilized. The lyophilized powder was dissolved in 50 mM Tris-HCl, pH 7.5, 100 mM KCl, 7M urea and applied to a Superdex 75 16/60 SEC column equilibrated in the same buffer. The protein containing fractions were collected, dialyzed, and lyophilized as described above. The lyophilized powder was stored at -20°C.

Single Stranded DNA (ssDNA) Preparation.

Poly 7 T ssDNA was purchased in 250 nmol form factor as a powder from Integrated DNA technologies pre-purified using IE HPLC. No further purification was done to the ssDNA. The DNA was dissolved into DI water to a concentration of 100 µM-150 µM and aliquoted into small volumes (50 µl) and stored at -20°C until use. Extinction coefficient of 8400 $M^{-1} \cdot m^{-1}$ per T nucleotide at 260 nm was used for concentration measurements.

Stock Buffer Preparation

A 10x concentration of working buffer (500 mM Tris-HCl, 1000mM NaCl, pH 7.5) was prepared, aliquoted into 50 mL tubes, and frozen. A 5% w/v Tween-20 in 1x concentration of working buffer was prepared, aliquoted into 1.7 mL tubes and frozen.

Stock Protein Sample Preparation

Stock protein samples were prepared by first diluting the 10x working buffer to 1x (50 mM Tris-HCl, 100mM NaCl, pH 7.5) and checking the pH. Protein powder was dissolved in approximately 1 mL of 1x working buffer and dialyzed overnight in the same buffer using a 3 kDa cutoff dialysis membrane at 4°C. The concentration was measured and adjusted to ~30µM using an extinction coefficient of 5,690 $M^{-1} \cdot m^{-1}$ at 280 nm. After the protein concentration was adjusted, the protein sample was aliquoted into ~250 µl fractions and frozen.

Sample Preparation for Fluorescence Experiments Without Osmolytes

Protein samples were made by taking one 250 µL protein solution aliquot and measuring the concentration one more time. 5% w/v Tween-20 was diluted to 0.05% w/v into the protein solution and the protein concentration was re-calculated based on the volume of added Tween-20 solution. Tween-20 addition was necessary to prevent adsorption of the protein to the plastic storage tubes. Adsorption causes problems at low protein concentrations when performing fluorescence experiments.

The protein sample containing Tween-20 was diluted to its final concentration of 0.3 µM. This was done by first preparing the buffer to be used for the fluorescence experiment. The buffer was prepared by diluting the 10x working buffer to 1x and adding and 0.05% Tween-20 into a 15 mL conical tube. Next, half of the volume of buffer was taken and the ~30 µM of protein was diluted to 0.3 µM into the buffer. This produced enough protein solution to perform 4-5 titrations.

DNA samples were prepared by diluting a 50 µL DNA aliquot to the ranges of ~5-10 µM, ~25-30 µM, and ~50-70 µM. This was done using enough DI water and 10x working buffer such that the DNA concentration reached the aforementioned target ranges. The concentration of diluted DNA solution was subsequently measured and was further adjusted as necessary. After the concentration was adjusted, 5% Tween-20 solution was diluted to 0.05% into the DNA solution and the DNA concentration was recalculated based on the volume of Tween-20 added.

Sample Preparation for Fluorescence Experiments with Osmolytes

The protein sample containing Tween-20 was diluted to its final concentration of 0.3µM. This was done by first preparing the buffer to be used for the fluorescence experiment. The buffer was prepared by diluting the 10x working buffer to 1x, diluting the 2.5 M sodium glutamate to 500 mM, 1 M, or 1.5 M, and diluting the 5% v/w Tween-20 to 0.05% w/v into a 15 mL conical tube. Next, half of the volume of buffer was taken and the ~30 µM of protein was diluted to 0.3 µM into the buffer. This produced enough protein and buffer solution to perform 4-5 titrations.

To ensure reasonable consistency between experiments, all of the sample dilutions for the fluorescence experiments were performed based on mass. Masses were obtained using an average of at least two measurements taken on an analytical balance. In all of the dilute solutions, it was

assumed that the density of the solution was approximately 1 g/cm^3; thus, the measured mass and volume were used interchangeably.

Fluorescence Spectroscopy

Fluorescence experiments were performed using a Horiba Fluoromax-4 spectrofluorometer. Temperature was controlled internally using a thermoelectric heater/cooler coupled to a cuvette holder. Fluorescence titrations were performed in a square 1 cm cuvette containing a stir bar. 1.5-1.7 mL of protein sample was used for each titration. DNA was added in 4 μL aliquots using a calibrated P10 micropipette. The total number of DNA additions was 15-20, and the protein sample dilution was kept below 5% over the course of each titration. Additions and spectral measurements were done under constant stirring. The protein-DNA mixture was allowed to stir for 4 minutes after each addition before recording a tryptophan emission spectrum. Tryptophan emission spectra were collected by exciting at 287 nm and collecting an emission spectrum from 320 to 500 nm. A buffer spectrum was recorded once before each titration. The raw emission spectra were buffer subtracted, averaged across 340 nm to 360 nm and plotted against the added DNA concentration. Each titration experiment was performed at least in triplicate.

Sample Preparation for High Pressure Fluorescence Experiments

All of the stock and working concentration buffers, protein solutions, and DNA solutions, with and without osmolytes, were prepared as described above. The difference between the high pressure and atmospheric experiments was that DNA could not be added in a similar manner to the atmospheric pressure titrations. Instead, pre-mixed protein-DNA samples were prepared and measured individually with varying concentrations of DNA. Samples were prepared by taking approximately 1 mL of 0.3 μM protein solution and diluting varying amounts of DNA into the protein sample. This produced enough sample to take three measurements in the high-pressure cell. 7-9 protein-DNA samples were prepared for each temperature or osmolyte condition. This was sufficient to cover the entire DNA titration range.

High Pressure Spectroscopy

High pressure experimental measurements were performed using an ISS high pressure cell fitted with sapphire windows on the Horiba Fluoromax-4 spectrofluorometer. The cell has five access ports on it. In our case, the top port is used to access the inside of the cell to load samples, purge the system of air, as well as to clean the interior. One of the side ports connects to the high pressure pump via high pressure piping. Two ports contain sapphire windowed plugs which are used for observation. The last window contains a blind plug. In this way, the high-pressure cell is set up in an "L" format for fluorescence experiments. The cell also has a built-in circulating water jacket that was connected to a thermostatic water bath to perform experiments at different temperatures.

Pressure was generated using a Pressure Biosciences Inc. HUB440 high pressure pump and was transduced using DI water. Pressure was ramped to 3,000 bars and down to 1 bar in 200 bar increments. Each pressure jump took 1 second to execute and a PID controller built into the pump made fine adjustments to ensure that the desired pressure was achieved within 30 seconds.

Approximately 300 μL of sample was placed in a specially made square quartz cuvette supplied by ISS. The cuvette was capped using a small piece of Dura Seal laboratory sealing film held in place with an o-ring. The sealing film allowed the pressure to be transduced into the cuvette and reduced sample leakage into the high pressure cell. The sample was equilibrated at each pressure for 5 minutes. Spectra were acquired once every 5 minutes. Fluorescence emission spectra were acquired by exciting at 287 nm and collecting an emission spectrum from 320 to 500 nm. Temperature was monitored and logged using a thermocouple probe attached to the HUB440 pump

and operated by the pump's software, or a probe attached to an Extech Instruments digital multimeter. Each experiment has been performed at least in triplicate.

Analysis of Ambient Pressure Binding Isotherms

To obtain the binding isotherms at atmospheric pressure, quenching of Tryptophan fluorescence intensity upon addition of ssDNA was monitored. The binding isotherms were analyzed according a binding model described below [13, 18]. The model assumes that one protein molecule will bind to one ssDNA molecule at equilibrium, as described by equation 2. In this equation $[N_f]$ and $[L_f]$ are the free protein and ligand concentrations; $[NL]$ is the concentration of the protein-ligand complex and it has a stoichiometry of 1.

$$[N_f] + [L_f] \rightleftharpoons [NL] \quad 2.$$

Based on the equilibrium described above, an equilibrium dissociation constant (K_d) can be determined according to equation 3.

$$K_d = \frac{[N_f][L_f]}{[NL]} \quad 3.$$

To calculate the K_d, the free concentrations of each of the three species will need to be known. They can be determined according to equations 4-6. Here, $[N_T]$ and $[L_T]$ refer to the total concentration of protein and ssDNA added.

$$[N_f] = [N_T] - [NL] \quad 4.$$
$$[N_T] = [NL] + [N_f] \quad 5.$$
$$[L_f] = [L_T] - [NL] \quad 6.$$

Substituting equations 4-6 into 3 and solving for $[NL]$ yields the following:

$$[NL] = \frac{([N_T] + [L_T] + K_d) - \sqrt{([N_T] + [L_T] + K_d)^2 - 4([N_T][L_T])}}{2} \quad 7.$$

This equation calculates the total concentration of the protein-ligand complex. From here this concentration can be written in terms of a fraction bound (F_b) according to 8.

$$F_b = \frac{[NL]}{[N_T]} \quad 8.$$

Equation **7** can be substituted into 8 to yield 9:

$$F_b = \frac{([N_T] + [L_T] + K_d) - \sqrt{([N_T] + [L_T] + K_d)^2 - 4([N_T][L_T])}}{2[N_T]} \quad 9.$$

This equation describes the fraction of ligand that is bound to the protein. However, it has no relation to the change in the observed signal. The following equation 10, relates the fraction bound to the fluorescence signal. Here, the I_N and I_{NL} refer to the theoretical maximum intensity of native protein and theoretical minimum intensities of protein ligand complex. I_{obs} refers to the observed fluorescence intensity.

$$F_b = \frac{(I_N - I_{obs})}{(I_N - I_{NL})} \quad 10.$$

Substituting equation 9 into 10 and solving for I_{obs} yields:

$$I_{obs} = I_N - \\ -(I_N - I_{NL}) \cdot \\ \cdot \frac{([N_T] + [L_T] + K_d) - \sqrt{([N_T] + [L_T] + K_d)^2 - 4([N_T][L_T])}}{2[N_T]} \quad 11.$$

This equation was used to simultaneously fit for I_N, I_{NL}, and K_d from the atmospheric pressure isotherms in order to get an equilibrium dissociation constant.

Analysis of High Pressure Protein Denaturation Isotherms

High pressure protein denaturation isotherms were analyzed according to a two-state model:

$$[N] \rightleftharpoons [U] \quad 12.$$

Based on this equation an unfolding equilibrium constant can be defined according as:

$$K_u = \frac{[U]}{[N]} \quad 13.$$

The unfolding equilibrium constant is related to protein stability and the pressure dependence of the stability as:

$$\Delta G_p = -RTln(K_u) \quad 14.$$

$$\Delta G_p = \Delta G^0_{Prot} + p\Delta V_{Prot} \quad 15.$$

Substituting 14 into 15 relates the unfolding equilibrium constant to the pressure dependence of stability as:

$$K_u = e^{\frac{\Delta G^0_{Prot} + p\Delta V_{Prot}}{-RT}} \quad 16.$$

Experimentally, signal intensities are related to the unfolding equilibrium constant according to 17, where I_{max} is the maximum theoretical intensity of the protein, and I_{obs} is the observed intensity.

$$K_u = \frac{(I_{max} - I_{obs})}{(I_{obs} - I_{min})} \quad 17.$$

Solving for I_{obs} in 17 and substituting 16 for K_u yields 18 which was used to fit the high-pressure denaturation isotherms.

$$I_{obs} = \frac{(I_{max} + I_{min}(e^{\frac{\Delta G^0_{Prot} + p\Delta V_{Prot}}{-RT}}))}{((e^{\frac{\Delta G^0_{Prot} + p\Delta V_{Prot}}{-RT}}) + 1)} \quad 18.$$

Analysis High Pressure Binding Isotherms using Thermodynamic Linkage Model

High pressure binding isotherms were analyzed according to the thermodynamic linkage model as given by Shriver and Edmondson [19]. Binding and stability can be described by the following linked equilibrium, where $[U_f]$, $[N_f]$, $[L_f]$, $[NL]$ are the free species of unfolded and native protein, DNA, and protein DNA complex at equilibrium, respectively. K_u describes the pressure dependence of the protein stability, K_{nl} describes the pressure dependence of binding. Here, we assume that ligand does not bind to the unfolded state:

$$[L_f] + [U_f] \overset{K_u}{\rightleftharpoons} [N_f] + [L_f] \overset{K_{nl}}{\rightleftharpoons} [NL] \quad 19.$$

In performing the binding experiments, we cannot directly measure the amount free ligand in solution. Thus, it needs to be calculated according to the following equation where $[L_T]$ is the total ligand added as:

$$\left[L_f\right] = [L_T] - [NL] \quad 20.$$

An overall binding polynomial (Q) and fractional populations of the native state (F_n), unfolded state (F_u) and bound state (F_{nl}) can be written as:

$$Q = 1 + K_u + K_{nl} \cdot \left[L_f\right] \quad 21.$$

$$F_n = \frac{1}{Q} \quad 22.$$

$$F_u = \frac{K_{un}}{Q} \quad 23.$$

$$F_{nl} = \frac{K_{nl} \cdot \left[L_f\right]}{Q} \quad 24.$$

The concentrations from equation 20 can be expressed as fractional concentrations by substituting 24 into 20 and rearranging to get 25, where $[N_T]$ is the total concentration of protein present.

$$0 = \left[L_f\right] - [L_T] - [N_T] \cdot F_{nl} \quad 25.$$

From here, the concentration of free ligand can be obtained by finding the root of 26**,** which yields to 26:

$$L_f = \frac{(K_{nl} \cdot [L_T] - 1 - K_u - [N_T] \cdot K_{nl})}{2 \cdot K_{nl}} + \\ + \frac{(\sqrt{((K_{nl} \cdot [L_T] - 1 - K_u - [N_T] \cdot K_{nl})^2) - (4 \cdot (-K_{nl}) \cdot ([L_T] + [L_T] \cdot K_u)}}{2 \cdot K_{nl}} \quad 26.$$

Thermodynamic parameters can then be obtained by solving for the equilibrium constant from the following equations 27 and 28 where ΔG_p is the stability at a particular pressure, $\Delta G^o$is the stability at atmospheric pressure, $\Delta V$is the volume change, R is the universal gas constant and T is the temperature in Kelvin and p is pressure in MPa.

$$\Delta G_p = \Delta G^o + p \cdot \Delta V \quad 27.$$

$$\Delta G_p = -R \cdot T \cdot \ln K(p) \quad 28.$$

solving for the equilibrium constant K yields to 29

$$K = e^{\frac{\Delta G^o + p \cdot \Delta V}{-R \cdot T}} \quad 29.$$

Substituting K from 29 with K_u or K_{nl} from 19 will yield thermodynamic information for the protein stability at atmospheric pressure (ΔG^o_{Prot}) and volume change upon unfolding at atmospheric pressure (ΔV_{Tot}) or binding stability (ΔG^o_{Bind}) and volume change upon binding at atmospheric pressure (ΔV_{Bind}), respectively as seen by equations 30 and 31:

$$K_u = e^{\frac{\Delta G^o_{Prot} + p \cdot \Delta V_{Prot}}{-R \cdot T}} \quad 30.$$

$$K_{nl} = e^{\frac{\Delta G^o_{Bind} + p \cdot \Delta V_{Bind}}{-R \cdot T}} \quad 31.$$

The system of equations from above can be related to the observed fluorescence intensities according to 32 where I_{obs} is the observed intensity, I_N is the theoretical maximum intensity from the protein in the native state, I_{NL} is the theoretical intensity from the protein ligand complex, and I_U is the theoretical fluorescence intensity from the unfolded state protein.

$$I_{obs} = I_N \cdot F_n + I_{NL} \cdot F_{nl} + I_U \cdot F_u \quad 32.$$

Finally, the fit of the system of equations was performed by simultaneously solving for the theoretical intensities (I_N, I_{NL}, I_U) as well as the thermodynamic parameters (ΔG^o_{Prot}, ΔV_{Prot}, ΔG^o_{Bind}, ΔV_{Bind}.).

Fits of the experimental data were performed using a nonlinear least square software package NLREG.

RESULTS

CspB-Bs binding to ssDNA at ambient pressure

CspB-Bs binding to single-stranded DNA template leads to a quenching of Trp8 fluorescence intensity and has been shown to be a useful proxy to monitor the binding reaction [13] upon titration of CspB-Bs solution with ssDNA template. It has been also established, that CspB-Bs preferentially binds single-stranded polypyrimidines with the highest affinity to the poly(T) single-stranded DNA (ssDNA) template [13]. Binding experiments established the size of the CspB-Bs binding site on polyDT to be 6-7 T-bases. This information was later used to solve the structure CspB-Bs in complex with hexa- and hepta-polypyrimidines [20]. Here, we used the hepta-deoxythimine (pDT7) to probe the effects of hydrostatic pressure on the thermodynamics of CspB-Bs:ssDNA interactions.

Figure 1 presents CspB-Bs:pDT7 isotherms obtained at ambient pressure (1 bar) and five different temperatures: 15°C, 20°C, 25°C, 31°C, and 37°C. The purpose for these experiments was to compare to our prior experiments performed mostly on longer ssDNA templates [12-14] as well as to establish a point of reference for the results of high-pressure experiments. Each isotherm was analyzed using equation 9 as described in the Methods section, and the resulting association constants, Ka, are listed in Table 1. From the inspection of the Ka values as a function of temperature, it is apparent that as the temperature is decreased, binding becomes much tighter, especially below 25°C. In the experiments below 25°C the binding appears to be "stoichiometric" where all pDT7 ssDNA template that is added becomes bound to the protein. The "breakpoint" of the low temperature isotherms occur at ~0.3 μM of total pDT7 added to the solution containing 0.3 μM CspB-Bs, and thus further corroborates the notion that CspB-Bs binding with the pDT7 ssDNA template has a binding stoichiometry of 1. The Ka values obtained here are in excellent agreement with the value reported previously [13]. For example, the Ka values obtained here at 25°C $(19\pm3)\cdot10^6$ M^{-1}, 31°C $(8\pm1)\cdot10^6$ M^{-1}, and at 37°C $(3\pm1)\cdot10^6$ M^{-1} are is in excellent agreement with the value of Ka(25°C)=$(24\pm1)\cdot10^6$ M^{-1}, Ka(31°C)=$(8\pm1)\cdot10^6$ M^{-1}, Ka(37°C)=$(4\pm1)\cdot10^6$ M^{-1}, reported by Lopez et. al. [13].

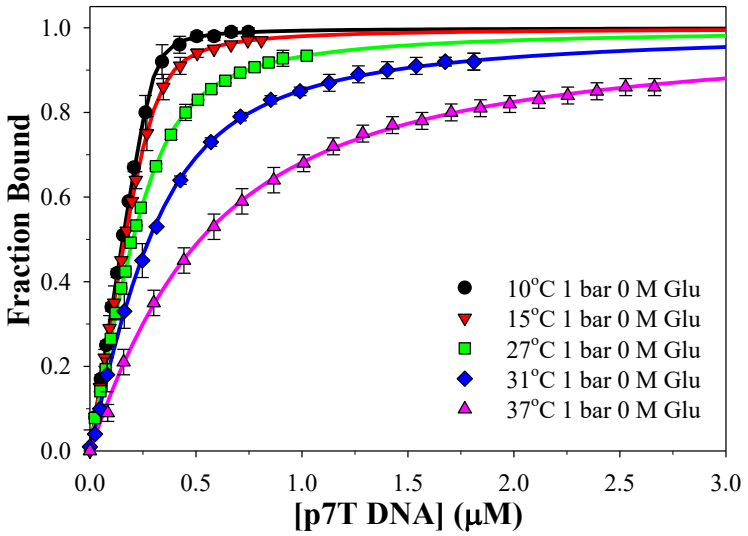

Figure 1. Binding isotherms for CspB-Bs with pDT7 ssDNA template at different temperatures, shown on the plot. Symbols show experimental data-points. The solid lines show the results of non-linear regression analysis of the data according to the Eq. 9, with the parameters listed in Table 1.

Effect of hydrostatic pressure on the stability of CspB-Bs

Having established the CspB-Bs binding at ambient pressure, we moved to characterizing the effects of hydrostatic pressure on the stability of CspB-Bs. To this end, we monitored changes in the tryptophan fluorescence intensity of CspB-Bs as a function of increase in pressure at three different temperatures: 15°C, 25°C, and 37°C (see Figure 2). With increase in pressure, the tryptophan fluorescence intensity decreases indicating that the protein is unfolding (note that the difference in the initial value of fluorescence intensity is due to the well-known effects of temperature on Trp-fluorescence). The pressure-induced unfolding was analyzed as described in the Methods section (see Eqs. 26-32). From the fit, we can obtain the stability of the protein at atmospheric pressure, ΔG^{o}_{Prot}, and the pressure dependence of stability, ΔV_{Prot}. These values are listed in Table 1. As expected, the increase in temperature leads to a decrease of CspB-Bs stability and this decrease is in excellent agreement with the previously reported values obtained from temperature or denaturant induced unfolding experiments [15]. The fact that CspB-Bs unfolds with increase of pressure indicates that ΔV_{Prot} is negative and is in good agreement with previously reported values. For comparison, the values for volume changes upon unfolding of CspB-Bs reported by the Schmid group [21-22] from urea (-43±5 ml/mol) or GdmSCN (-42±12 ml/mol) induced unfolding at 25°C at different pressures agrees well with our estimates (-35±4 ml/mol). Furthermore, the ΔV_{Prot}=-40±5 ml/mol, predicted from our previously published computational algorithm [1, 3] also compares well with the experimental values. The negative value of the ΔV_{Prot} for CspB-Bs is consistent with negative ΔV_{Prot} of many other proteins, suggesting the majority of protein become unstable upon increase in hydrostatic pressure. The midpoint pressure of unfolding transition (e.g. pressure at which ΔG^{o}_{Prot}=0) for CspB-Bs at 37°C is ~1,700 bars well within 1-3000 bar range of our experimental setup.

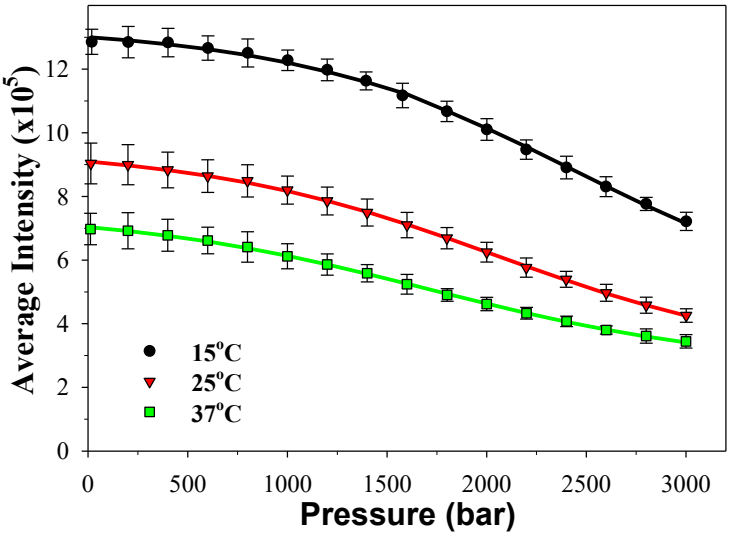

Figure 2. Dependence of the averaged fluorescence intensity at 350 nm on hydrostatic pressure for CspB-Bs in solution at different temperatures, shown on the plot. Symbols show experimental data-points. The solid lines show the results of non-linear regression analysis of the data according to the Eq. 18, with the parameters listed in Table 1.

CspB-Bs binding to ssDNA at high hydrostatic pressure

Having characterized the DNA binding affinity of CspB-Bs at atmospheric pressure, as well as the pressure dependence of CspB-Bs stability, we next performed the high-pressure CspB-Bs:DNA binding experiments. Based on the atmospheric pressure titration isotherms, we chose three temperatures: 25°C, 31°C, and 37°C shown in Figure 3. Direct titration are not possible due to the obvious problems of delivering the titrant into pressurized high-pressure cell. Thus, these experiments are performed by premixing CspB-Bs with different amounts of DNA and measuring the fluorescence intensity at a constant temperature as a function of hydrostatic pressure. The fluorescence intensity as a function of pressure was collected from both pressure ramp-up and down thus resulting in two data sets per experiment. Each experiment was repeated in triplicate. Since increase in hydrostatic pressure leads to CspB-Bs unfolding and will also affect the CspB-Bs:pDT7 binding, the isotherms obtained at different CspB-Bs:pDT7 ratios were combined and analyzed using a thermodynamic linkage model as described in the Methods section (Eqs. 26-32). The linkage model accounts for two linked equilibria: CspB-Bs folding/unfolding equilibrium as function of pressure and the binding equilibrium of native CspB-Bs to pDT7 ssDNA template as a function of pressure.

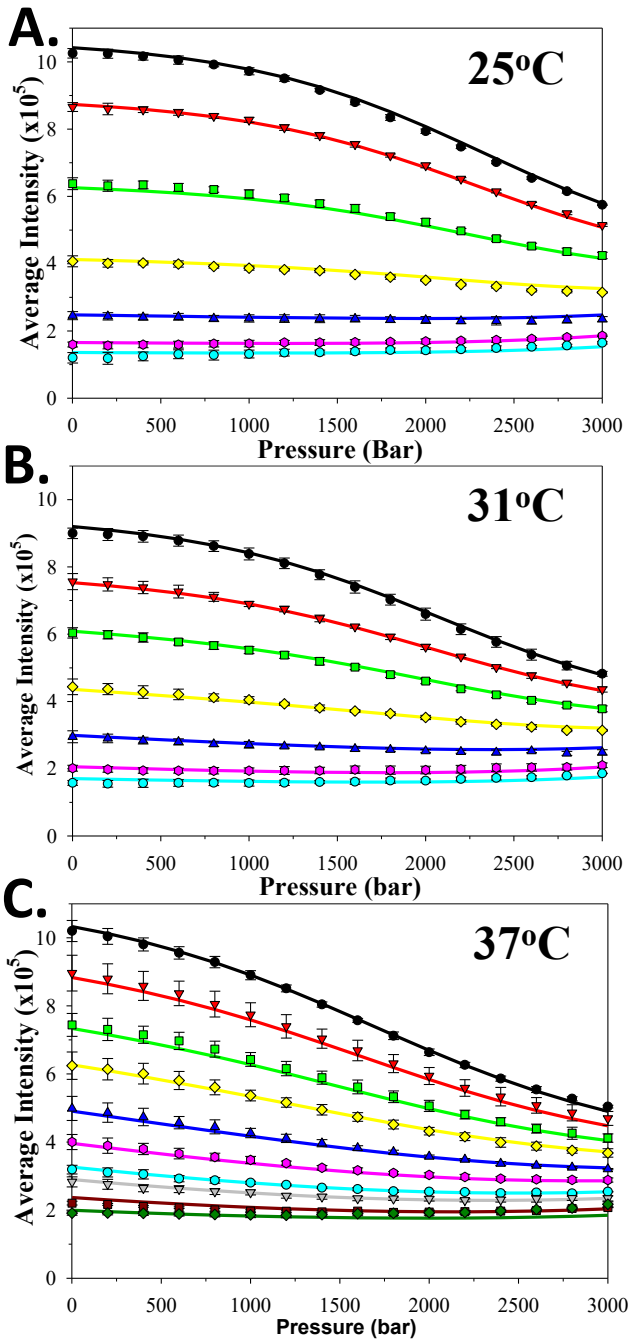

Figure 3. Dependence of the averaged fluorescence intensity at 350 nm on hydrostatic pressure for CspB-Bs in solution in the presence of different concentrations of pDT7 ssDNA template: **Panel A.** Experiments performed at 25°C: ● 0 μM DNA, ▼ 0.06 μM, ■ 0.16 μM, ♦ 0.26 μM, ▲ 0.41 μM, ⬣ 0.65 μM, ● 0.94 μM. **Panel B.** Experiments performed at 31°C: ● 0 μM DNA, ▼ 0.09 μM, ■ 0.17 μM, ♦ 0.31 μM, ▲ 0.52 μM, ⬣ 0.93 μM, ● 1.40 μM. **Panel C.** Experiments performed at 37°C: ● 0 μM DNA, ▼ 0.09 μM, ■ 0.20 μM, ♦ 0.30 μM, ▲ 0.48 μM, ⬣ 0.68 μM, ● 0.92 μM, ▼ 1.11 μM, ■ 1.56 μM, ♦ 2.70 μM. The solid lines show the results of non-linear regression analysis of the data according to the Eqs. 26-32, with the parameters listed in Table 1.

The global analysis to a thermodynamic linkage model provides estimates of 4 thermodynamics parameters at a given temperature: the stability of CspB-Bs at ambient pressure, ΔG^o_{Prot}, the volume change upon CspB-Bs unfolding, ΔV_{Prot}, the association constant for CspB-Bs:pDT7 complex at ambient pressure, K^o_a, and the volume changes upon pDT7 ssDNA template binding, ΔV_{Bind}. These parameters are listed in Table 1.

Validation of thermodynamic parameters

To validate self-consistency of the thermodynamic linkage analysis, a number of comparisons were made. Figure 4 shows comparison of the ΔG^o_{Prot} obtained from the pressure induced unfolding of CspB-Bs in the absence (shown in Figure 2) and presence of the pDT7 ssDNA template (shown in Figure 3) and previously published temperature dependence of ΔG^o_{Prot} [15]. The agreement is quite remarkable, particularly at higher temperatures. This is because higher net stability at lower temperatures make protein more resistant to pressure-induced unfolding. As a result, due to the technical limitation on the upper limit of pressures that can be achieved in the experiments, a more limited part of the transition is attained. This, in turn, leads to larger uncertainties in the estimates of ΔG^o_{Prot}. At 15°C, the midpoint pressure of unfolding transition (e.g. pressure at which ΔG^o_{Prot}=0) for CspB-Bs in the absence of the pDT7 ssDNA template is ~2,500 bars, which is close to the upper limit of pressure that can be achieved in the high-pressure optical cell. However, at 37°C, the midpoint of transition drops to ~1,700 bars, and thus almost the complete transition is observed.

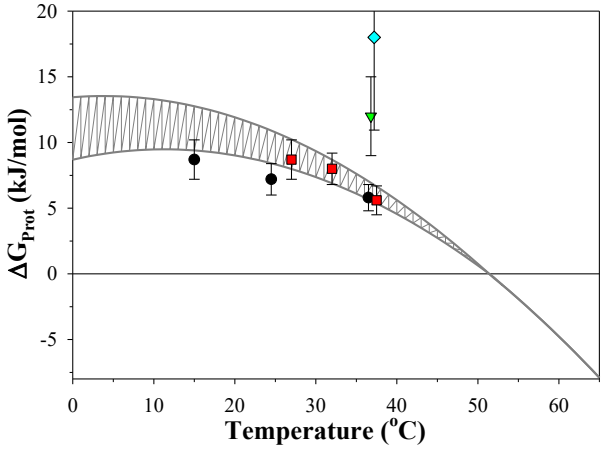

Figure 4. Temperature-dependence of the Gibbs energy of unfolding for CspB-Bs, ΔG_{Prot}. The continuous lines enclosing the shaded area are taken from [15]. Symbols show the ΔG_{Prot} values obtained from pressure induced unfolding experiment described in present work (see also Table 1): ● - black circles are from the pressure-induced unfolding experiments on CspB-Bs in the absence of ssDNA shown in Figure 2; ■ red squares are from the pressure-induced unfolding experiments of CspB-Bs in the presence of ssDNA, shown in Figure 3 ▼ green down triangles and ♦ cyan diamonds are from the pressure-induced unfolding experiments of CspB-Bs in the presence of ssDNA in addition to 0.5 M or 1.5 M Glu, respectively, shown in Figure 7.

Figure 5 compares the volume change upon CspB-Bs unfolding, ΔV_{Prot}, obtained from the pressure induced unfolding of CspB-Bs in the absence (shown in Figure 2) and presence of the pDT7 ssDNA template (shown in Figure 3). Again, the agreement between the ΔV_{Prot} values

obtained from these two different sets of data analyzed using different models is remarkable. Furthermore, the values of the association constant for CspB-Bs:pDT7 complex at ambient pressure, K_a^o, obtained from the thermodynamic linkage analysis of high pressure data and direct titrations at ambient pressure are similarly very good. For example, the K_a^o at 37°C obtained from the linkage analysis $(5\pm3)\cdot10^6$ M^{-1} agrees well with the value of $(3\pm1)\cdot10^6$ M^{-1} obtained from the direct titration.

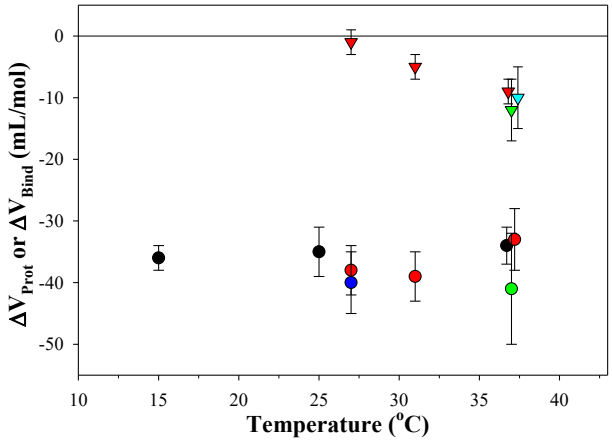

Figure 5. Temperature-dependence of the volume changes unfolding for CspB-Bs, ΔV_{Prot}, and the volume changes upon CspB-Bs:pDT7 ssDNA tempalate binding, ΔV_{Bind}. The circles show the values of ΔV_{Prot} and triangles are for ΔV_{Bind} (see Table 1 for numerical values). Color-coding is as follows: black symbols are obtained from the pressure-induced unfolding experiments on CspB-Bs in the absence of ssDNA shown in Figure 2; red symbols are the values obtained from the pressure-induced unfolding experiments on CspB-Bs in the presence of ssDNA shown in Figure 3; green and cyan symbols are the values obtained from the pressure-induced unfolding experiments of CspB-Bs in the presence of ssDNA in addition to 0.5 M or 1.5 M Glu, respectively, shown in Figure 7. Blue circle shows the volume changes of CspB-Bs unfolding predicted based on the computational modeling [1].

The agreement between three parameters, ΔG_{Prot}^o, ΔV_{Prot}, and K_a^o obtained from high-pressure experiments in the absence and presence of the pDT7 ssDNA template at 37°C or from direct titration of CspB-Bs with pDT7 lends credibility to the estimates of ΔV_{Bind}, the only parameter that cannot be validated from the experiments presented above. The ΔV_{Bind} values obtained from the linkage analysis of high-pressure data for CspB-Bs binding to pDT7 ssDNA template as a function of temperature are shown in Figure 3. It evident that the volume changes upon binding are small in magnitude and negative. This negative binding volume indicates that the total volume of the complex is smaller than the sum of the component volumes of the CspB-Bs and the ssDNA - (i.e. the volume of the non-bound state). This suggest that the binding affinity will ***increase*** with increase in hydrostatic pressure.

This result is highly unexpected, as there is a trove of published data suggesting that volume changes upon protein binding to DNA (to the best of our knowledge the data is limited to protein-double stranded DNA interactions) is positive, i.e. the binding affinity will ***decrease*** with increase in hydrostatic pressure [23-27].

Thus one cannot exclude the possibility that the negative ΔV_{Bind} is an artefact of our data analysis. To this end, we recognize that the low stability of CspB-Bs is a major obstacle to direct

observation of CspB binding at high pressure. Thus, we turned to stabilizing osmolytes that are known to increase protein stability [28-35]. Interestingly, the effects of osmolytes on protein stability does not have effect on the volume changes upon protein unfolding [36]. It is also well known that the osmolytes also increase the binding affinity of protein-DNA complexes. This is true for the CspB-Bs binding to pDT7 ssDNA template. Figure 6 shows the binding isotherms for CspB-Bs binding to pDT7 obtained at 37°C in the presence of increasing concentrations of glutamate, one of the stabilizing osmolytes that has been shown in our previous study to have no effect on the volume changes upon protein unfolding [36]. It is clear that addition of 0.5 M, 1.0 M and 1.5 M glutamate progressively increases binding affinity at ambient pressure from $(3\pm1)\cdot10^6$ M^{-1} in 0 M glutamate to $(13\pm1)\cdot10^6$ M^{-1} in 1.5 M glutamate. This increase in binding affinity upon addition of 1.5 M glutamate is equivalent to an increase in binding affinity upon lowering temperature by 6-7 degrees.

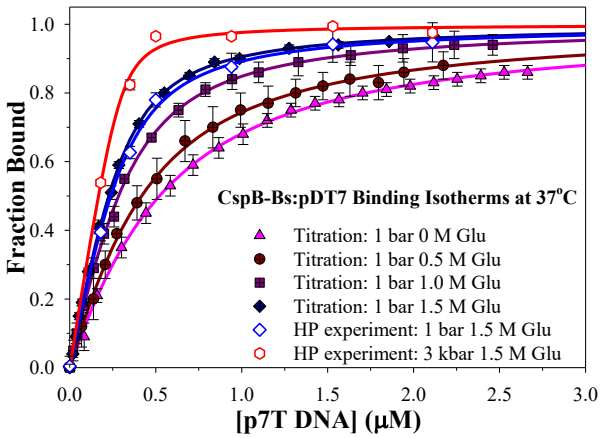

Figure 6. Binding isotherms for CspB-Bs with pDT7 ssDNA template at 37°C in the presence of different concentrations of glutamate, shown on the plot. Solid symbols show experimental data-points obtained from direct titration at 1 bar, while open symbols show the experimental data-points obtained from HP experiments at 1 bar (◊) and 3000 bars (○). The solid lines show the results of non-linear regression analysis of the data according to the Eq. 9, with the parameters listed in Table 1.

We next performed the high-pressure CspB-Bs:pDT7 binding experiments at 37°C in the presence of 0.5 M glutamate. Figure 7A shows the results of these experiments that were again analyzed using the linkage model (Eqs. 26-32), to obtain the four thermodynamic parameters at this temperature in the presence of osmolyte (see Table 1). Based on the binding isotherms obtained at ambient pressure and the well-established general effects of osmolytes on protein stability, there is an increase in ΔG^o_{Prot} and an increase in K^o_a This agrees well with our previous study on the effects of osmolytes on the volume changes [36], and shows no significant changes in ΔV_{Prot} or ΔV_{Bind}. Importantly, the latter remains negative. From the values of ΔG^o_{Prot} and ΔV_{Prot} we can deduce that the midpoint pressure of unfolding transition, upon addition of 0.5 M glutamate, will increase from ~1,700 bars to ~3,000 bar. The concentration-dependent, osmolyte-induced stability enhancement ensures that the protein remains in its native state throughout the experimentally accessible pressure range which eliminates the need to use the linkage model for analysis. This allows us to directly obtain binding isotherms at different pressures.

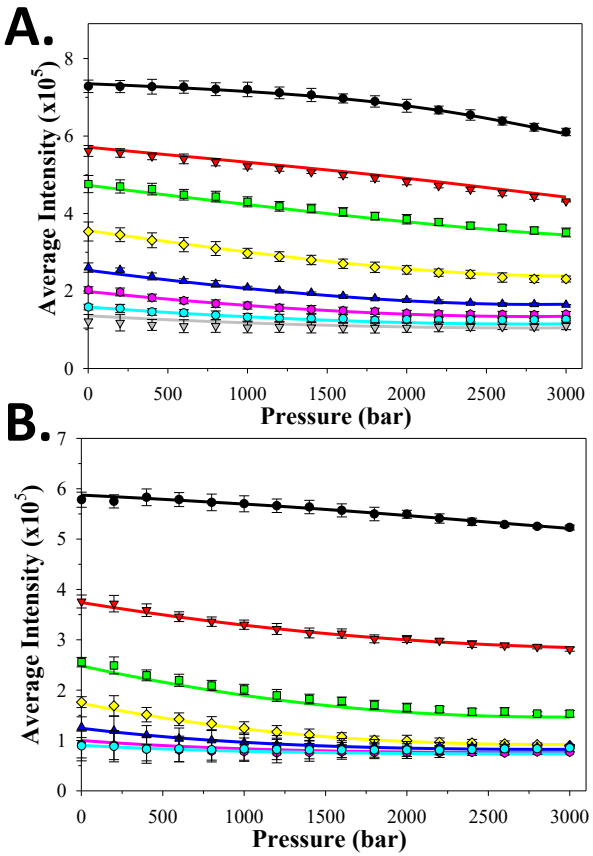

Figure 7. Dependence of the averaged fluorescence intensity at 350 nm on hydrostatic pressure at 37°C for CspB-Bs in solution in the presence of different concentrations of pDT7 ssDNA template: **Panel A.** Experiments performed at 37°C in the presence of 0.5 M Glu: ● 0 μM DNA, ▼ 0.13 μM, ■ 0.23 μM, ♦ 0.40 μM, ▲ 0.68 μM, ⬣ 1.00 μM, ● 1.50 μM, ▼ 2.10 μM. **Panel B.** Experiments performed at 37°C in the presence of 1.5 M Glu: ● 0 μM DNA, ▼ 0.18 μM, ■ 0.35 μM, ♦ 0.50 μM, ▲ 0.94 μM, ⬣ 1.53 μM, ● 2.11 μM. The solid lines show the results of non-linear regression analysis of the data according to the Eqs. 26-32, with the parameters listed in Table 1.

Figure 7B shows the results of high-pressure CspB-Bs:pDT7 binding experiments at 37°C in the presence of 1.5 M glutamate. Under these conditions, the protein remains folded in the entire experimental pressure range. Thus, we can directly construct the binding isotherms at different pressures and analyze them without using a linkage model. Figure 6 compares 37°C binding isotherm for CspB-Bs:pDT7 complex at ambient pressure in the presence of 1.5 M glutamate obtained from the direct titration and from the high-pressure experiments (i.e. analyzing the values fluorescence intensity at 1 bar from high pressure experiments). The two data sets agree remarkably well. Figure 6 also shows the binding isotherm obtained from the analysis of the fluorescence intensity at 3000 bar from the high pressure experiments. It is evident that the binding affinity at high pressure is much higher than at low pressure, $(11\pm2)\cdot10^6$ M^{-1} versus $(58\pm8)\cdot10^6$ M^{-1}. This validates the results obtained from the thermodynamic linkage analysis of the pressure induced unfolding in the absence of glutamate, namely that the ΔV_{Bind} is negative.

The only other (to the best of our knowledge) report of the protein-ssDNA system at high pressure is that of Merrin et. al. [37]. In their study, the authors compared the effects of pressure and temperature on ssDNA binding using RecA proteins from *Escherichia coli* (EC-RecA) and *Thermus thermophilus* (TT-RecA). The experimental setup was to monitor the changes in fluorescence anisotropy of labeled ssDNA in the presence of RecA proteins at one fixed ssDNA/RecA ratio as a function of pressure at different temperatures. The anisotropy of EC-RecA/ssDNA showed sigmoidal transition upon increase in pressure, while signal for the ssDNA/TT-RecA did not show such transition. They attributed the observed transition to dissociation and reported volume changes for EC-RecA binding to ssDNA to be large and positive (~200 ml/mol), implying that binding affinity decreases with the increase in pressure. The effects of hydrostatic pressure on the intrinsic stability of RecA was not performed, although the authors did entertain this possibility. Thus, because thermodynamics of ssDNA binding and protein stability are linked phenomena, a linkage analysis of their data will be necessary to deconvolute each component, and provide a definite value for the sign and magnitude of volume changes upon ssDNA binding in EC-RecA system.

DISCUSSION

The high-pressure binding study presented here used the cold shock protein B from *Bacillus subtilis* and studied the pressure effects on its ability to bind single stranded polyT DNA. Extensive high-pressure experimental data collected at different protein:ssDNA ratios and different temperatures was analyzed using a thermodynamic linkage model, that accounts for both protein unfolding and protein:ssDNA binding [19]. In the simplest form, protein (CspB-Bs) can bind ligand (ssDNA) only in the folded form, and thus binding equilibrium will affect the folding:unfolding equilibrium. For the same reason, protein folding will affect the protein-ligand equilibrium by increasing the concentration of binding-competent protein and thus increasing the fraction of protein-ligand complexes. The equilibrium for individual processes, folding and binding, can react differently to external perturbation by high hydrostatic pressure thus leading to a complex behavior. The protein, CspB-Bs, unfolds with increase in hydrostatic pressure. This is because the volume changes upon unfolding ΔV_{Prot} are large in absolute value and negative. Our study showed that the binding reaction has a small in magnitude but negative ΔV_{Bind} value. This means that the binding of CspB-Bs to ssDNA is stabilized by increase in hydrostatic pressure. Thus, we have a case of linked equilibria, in which the two elementary steps, folding and binding, react in the opposite directions upon increase in hydrostatic pressure. The protein folding/unfolding equilibrium favors unfolded state, while protein-ligand binding favors bound state, which can only occur when the protein is folded.

Importantly, the ΔV_{Bind} appears to become more negative with increase in temperature suggesting binding will become even more favorable at higher pressures and temperatures. This means that the binding of pDT7 ssDNA to CspB-Bs itself is not prone to destabilization at high pressures as it is inherently pressure-stable. In fact, in the presence of ligand, the binding reaction will be stabilized by the application of pressure. However, due to the fact that the protein itself is not pressure-stable it will eventually unfold at high pressures rendering it incapable of binding. From a thermodynamic perspective, these opposing effects act against each other to effectively set a "maximum attainable" pressure tolerance to the protein-ssDNA complex under given conditions.

Our study also showed us that this "maximum" can be further enhanced by introducing stabilizing osmolytes such as glutamate. Glutamate significantly stabilizes the protein against effects of high pressure without affecting its ΔV_{Prot} which allows the protein to remain in its native,

binding-competent state at much higher pressures. Given that binding is not negatively affected by pressure, this enables binding to take place at the previously prohibitive pressures. Moreover, glutamate also slightly stabilizes the binding reaction without affecting the ΔV_{Bind} which works in concert to further increase the pressure tolerance of the protein-DNA complex.

Having characterized the protein-DNA binding, we can use the analysis model and the derived parameters and simulate the binding data, in order to gain a better understanding of how protein DNA complex will behave in an extended range of pressures. Figure 8 shows 3D reconstructed surfaces where pressure and DNA concentrations are on the x and y axes, the fraction of bound protein and fraction of free native protein are depicted on the z axis. The surfaces were generated using fitted parameters obtained from the high-pressure protein-DNA binding experiments listed in Table 1. Even though the experimental conditions only achieved pressure up to 3000 bar, the simulated surfaces show pressure up to 10,000 bars where complete unfolding of the protein is achieved. As can be seen from Figure 8A, as pressure increases the protein begins to unfold and the fractions of native and bound are depleted. However, as DNA is added, the native and bound fractions increase, and the surface expands towards higher pressures, at increasing concentrations of DNA. Furthermore, as temperature is increased, the overall fraction of native and bound decreases, indicating that temperature destabilizes both the protein and the protein DNA complex. Addition of 0.5 M (Figure 8B) and 1.5 M (Figure 8C) osmolyte progressively stabilizes both CspB-Bs and CspB-BS:pDT7 complex. In 1.5 M osmolyte (Figure 8C), CspB-Bs is expected to be stable at the pressures as high at 4000 bars. Addition of pDT7 ssDNA template will further increase the faction of native CspB-Bs. However, because of the large absolute value of ΔV_{Prot} than ΔV_{Bind}, the fraction of native CspB-Bs will eventually start to decrease, but this decrease will occur at much higher pressures than in the absence of osmolyte.

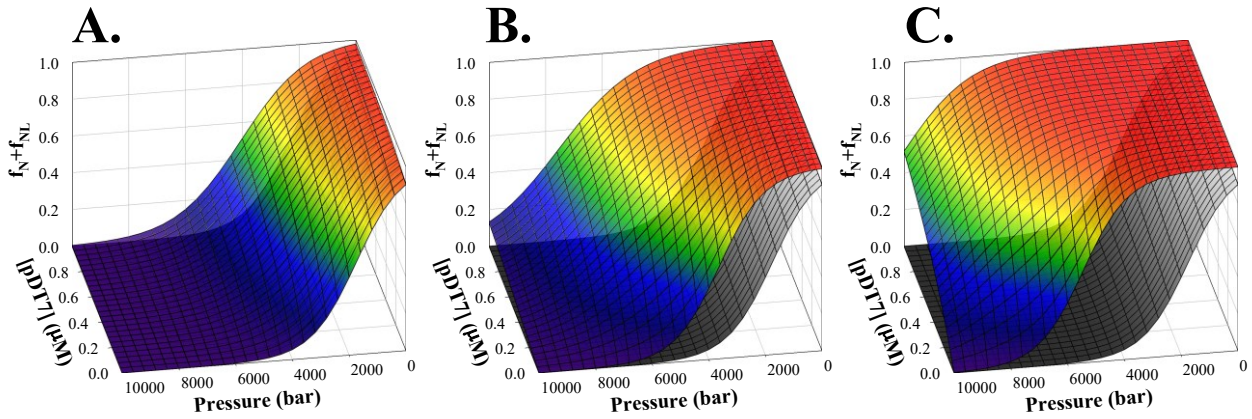

Figure 8. CspB-Bs:pDT7 binding as a function of pressure and DNA concentration. The surfaces show the total fraction of native CspB-Bs, i.e. fractions of bound and free native protein, Fnl+Fn. The surfaces are computed based on the Eqs. 26-32 with the parameters taken from Table 1. **Panel A.** CspB-Bs:pDT7 binding at 37°C 0 M Glu; **Panel B.** CspB-Bs:pDT7 binding at 37°C 0.5 M Glu; **Panel C.** CspB-Bs:pDT7 binding at 37°C 1.5 M Glu. On each of the three panel, gray surface for CspB-Bs in the absence of DNA is shown for comparison.

Given our experimental findings about the pressure-dependent binding properties of CspB-Bs from *Bacillus subtilis*, it may be tempting to generalize these observations to all Csp's. This is because cold shock proteins accomplish their binding to single stranded nucleic acids using the

highly conserved RNP1 and RNP2 motifs [16]. This common feature may imply that the functions of these proteins are redundant; however, there is a body of evidence suggesting that a subset of these proteins have unique function.

Indeed, the unique nature of these proteins can be surmised by the fact that they are expressed not only upon cold shock, but also constitutively and during other stress inducing conditions. Moreover, cold shock proteins are also known to have an affinity to specific sequences [12-14, 38]: CspB binds to U-rich regions of ssRNA, CspC binds to GA regions, and CspE preferentially binds to AU regions. Functionally, in *E. coli* CspE is known to inhibit anti-termination by binding to the mRNA and preventing formation of secondary structure while CspA, CspB, and CspC lack anti-termination function [39]. Csp's can also regulate the expression of proteins in a concentration dependent manner by binding to the loop regions of mRNA in order to prevent secondary structure formation [40] thus inhibiting translation of mRNA due to the formation of dsRNA segments. This will also increase the lifetime of mRNA by protecting them for RNases that specifically degrade dsRNA [16, 40].

With this consideration in mind, it will be important to study the pressure dependent binding properties of Csp's from different sources that have varying affinity to different nucleic acid sequences as their binding may exhibit differing pressure stabilities. It possible that a subset of Csp's exhibiting pressure-stable binding are overexpressed or expressed constitutively in the high-pressure environment, while proteins without such characteristics are not. Certainly, this possibility is not without merit as it was shown that the facultative psychropiezophile *Photobacterium profundum* changes its gene-expression profile in a pressure dependent manner [41]. Future studies of binding specificity of Csp's from different organisms will be able to provide more details on such functionality at elevated pressure.

ACCESSION CODES

CspB-Bs: UniProtKB P32081

Table 1. Thermodynamic Parameters of CspB-Bs and CspB-Bs:pDT7 complex.

Temperature [Glutamate]	ΔG_{Prot} (kJ/mol)	ΔV_{Prot} (mL/mol)	ΔG_{Prot} (kJ/mol)	ΔV_{Prot} (mL/mol)	K_a ($x10^6$ M^{-1})	K_a ($x10^6$ M^{-1})	ΔV_{Bind} (mL/mol)
15°C	8.6±0.4 [a]	-36±2 [a]	nd	nd	215±53 [c]	nd	nd
21°C	nd	nd	nd	nd	71±22 [c]	nd	nd
25°C	7.2±0.9 [a]	-35±4 [a]	8.7±0.8 [b]	-38±4 [b]	19±3 [c]	33±12 [b]	-1±2 [b]
31°C	nd	nd	8.0±0.8 [b]	-39±4 [b]	8±1 [c]	12±8 [b]	-5±2 [b]
37°C	5.8±0.8 [a]	-34±3 [a]	5.6±1.1 [b]	-33±5 [b]	3±1 [c]	5±3 [b]	-9±2 [b]
37°C 0.5 M	nd	nd	12±3 [b]	-41±9 [b]	4±1 [c]	6±4 [b]	-12±5 [b]
37°C 1.5 M	nd	nd	>16 [b]	nd	13±1 [c]	11±2 [d]	-11±6 [e]

[a] Obtained from the fit of data shown in Figure 2 to the Eq. 18;
[b] obtained from the fit of data shown in Figures 3 and 7A to the Eqs. 26-32;
[c] obtained from the fit of data shown in Figures 1 and 6 to the Equation 9;
[d] obtained from the fit of data at 1 bar shown in Figure 7B to the Equation 9;
[e] obtained from the fit of data at each pressure shown in Figure 7B to the Equation 9, and calculating the ΔV_{Bind} from the slope of ΔG_{Bind}=-RTln(Ka) dependence of pressure.

All uncertainties are the 95% confidence intervals of non-linear regression fit.

AUTHOR INFORMATION

Corresponding Author

George I. Makhatadze - *Departments of Biological Sciences, and Chemistry and Chemical Biology, Center for Biotechnology and Interdisciplinary Studies, Rensselaer Polytechnic Institute, Troy, NY 12180, USA*; Phone: (518)276-4417; Email: makhag@rpi.edu orcid.org/0000-0003-4565-1264

Authors

Samvel Avagyan - *Department of Biological Sciences, Center for Biotechnology and Interdisciplinary Studies, Rensselaer Polytechnic Institute, Troy, NY 12180, USA.*

Author Contributions

S.A. performed all experiments. S.A. and G.I.M. designed and analyzed experiments and wrote the paper.

Funding Sources

This work was supported by a grant CHEM/CLP-1803045 (to G.I.M.) from the US National Science Foundation (NSF).

Notes

The authors declare no competing financial interest.

ACKNOWLEDGEMENTS

We thank Dr. Alexander Lazarev (Pressure Bioscience) for help with automation and interfacing of high-pressure pump and Dr. Catherine Royer (RPI) for suggestions related to fluorescence measurements.

REFERENCES

1. Chen, C. R.; Makhatadze, G. I. Molecular determinant of the effects of hydrostatic pressure on protein folding stability. *Nature Communications* **2017,** *8*, 14561.
2. Avagyan, S.; Vasilchuk, D.; Makhatadze, G. I. Protein adaptation to high hydrostatic pressure: Computational analysis of the structural proteome. *Proteins: Structure, Function, and Bioinformatics* **2019,** *88*, 584-592.
3. Chen, C. R.; Makhatadze, G. I. ProteinVolume: calculating molecular van der Waals and void volumes in proteins. *BMC Bioinformatics* **2015,** *16*, 101-107.
4. Yayanos, A. A.; Pollard, E. C. A study of the effects of hydrostatic pressure on macromolecular synthesis in Escherichia coli. *Biophys J* **1969,** *9*, 1464-1482.
5. Kato, C.; Sato, T.; Smorawinska, M.; Horikoshi, K. High pressure conditions stimulate expression of chloramphenicol acetyltransferase regulated by the lac promoter in Escherichia coli. *FEMS Microbiology Letters* **1994,** *122*, 91-96.
6. Royer, C. A.; Weber, G.; Daly, T. J.; Matthews, K. S. Dissociation of the lactose repressor protein tetramer using high hydrostatic pressure. *Biochemistry* **1986,** *25*, 8308-8315.
7. Pope, D. H.; Smith, W. P.; Swartz, R. W.; Landau, J. V. Role of bacterial ribosomes in barotolerance. *Journal of Bacteriology* **1975,** *121*, 664.
8. Gross, M.; Lehle, K.; Jaenicke, R.; Nierhaus, K. H. Pressure-induced dissociation of ribosomes and elongation cycle intermediates. *European Journal of Biochemistry* **1993,** *218*, 463-468.
9. Oger, P. M.; Jebbar, M. The many ways of coping with pressure. *Research in Microbiology* **2010,** *161*, 799-809.
10. Levin, A.; Cinar, S.; Paulus, M.; Nase, J.; Winter, R.; Czeslik, C. Analyzing protein-ligand and protein-interface interactions using high pressure. *Biophys Chem* **2019,** *252*, 106194.
11. Son, I.; Shek, Y. L.; Dubins, D. N.; Chalikian, T. V. Volumetric characterization of tri-N-acetylglucosamine binding to lysozyme. *Biochemistry* **2012,** *51*, 5784-5790.
12. Lopez, M. M.; Makhatadze, G. I. Major cold shock proteins, CspA from Escherichia coli and CspB from Bacillus subtilis, interact differently with single-stranded DNA templates. *Biochimica et Biophysica Acta (BBA) - Protein Structure and Molecular Enzymology* **2000,** *1479*, 196-202.
13. Lopez, M. M.; Yutani, K.; Makhatadze, G. I. Interactions of the Major Cold Shock Protein of Bacillus subtilis CspB with Single-stranded DNA Templates of Different Base Composition. *Journal of Biological Chemistry* **1999,** *274*, 33601-33608.
14. Lopez, M. M.; Yutani, K.; Makhatadze, G. I. Interactions of the Cold Shock Protein CspB fromBacillus subtilis with Single-stranded DNA: Importance of the T-base Content and Position with the Template. *Journal of Biological Chemistry* **2001,** *276*, 15511-15518.
15. Makhatadze, G. I.; Loladze, V. V.; Gribenko, A. V.; Lopez, M. M. Mechanism of Thermostabilization in a Designed Cold Shock Protein with Optimized Surface Electrostatic Interactions. *Journal of Molecular Biology* **2004,** *336*, 929-942.
16. Ermolenko, D. N.; Makhatadze, G. I. Bacterial cold-shock proteins. *Cellular and Molecular Life Sciences* **2002,** *59*, 1902-1913.
17. Murzin, A. G. OB(oligonucleotide/oligosaccharide binding)-fold: common structural and functional solution for non-homologous sequences. *EMBO J* **1993,** *12*, 861-867.
18. Wyman, J.; Gill, S. J., *Binding and linkage: functional chemistry of biological macromolecules*. University Science Books: 1990.

19. Shriver, J. W.; Edmondson, S. P. Ligand-binding interactions and stability. *Methods Mol Biol* **2009,** *490*, 135-164.
20. Sachs, R.; Max, K. E.; Heinemann, U.; Balbach, J. RNA single strands bind to a conserved surface of the major cold shock protein in crystals and solution. *RNA* **2012,** *18*, 65-76.
21. Jacob, M.; Holtermann, G.; Perl, D.; Reinstein, J.; Schindler, T.; Geeves, M. A.; Schmid, F. X. Microsecond folding of the cold shock protein measured by a pressure-jump technique. *Biochemistry* **1999,** *38*, 2882-2891.
22. Jacob, M. H.; Saudan, C.; Holtermann, G.; Martin, A.; Perl, D.; Merbach, A. E.; Schmid, F. X. Water contributes actively to the rapid crossing of a protein unfolding barrier. *J Mol Biol* **2002,** *318*, 837-845.
23. Robinson, C. R.; Sligar, S. G. Heterogeneity in molecular recognition by restriction endonucleases: osmotic and hydrostatic pressure effects on BamHI, Pvu II, and EcoRV specificity. *Proc Natl Acad Sci U S A* **1995,** *92*, 3444-3448.
24. Robinson, C. R.; Sligar, S. G. Changes in solvation during DNA binding and cleavage are critical to altered specificity of the EcoRI endonuclease. *Proc Natl Acad Sci U S A* **1998,** *95*, 2186-2191.
25. Royer, C. A.; Chakerian, A. E.; Matthews, K. S. Macromolecular binding equilibria in the lac repressor system: studies using high-pressure fluorescence spectroscopy. *Biochemistry* **1990,** *29*, 4959-4966.
26. Senear, D. F.; Tretyachenko-Ladokhina, V.; Opel, M. L.; Aeling, K. A.; Hatfield, G. W.; Franklin, L. M.; Darlington, R. C.; Alexander Ross, J. B. Pressure dissociation of integration host factor-DNA complexes reveals flexibility-dependent structural variation at the protein-DNA interface. *Nucleic Acids Res* **2007,** *35*, 1761-1772.
27. Silva, J. L.; Silveira, C. F. Energy coupling between DNA binding and subunit association is responsible for the specificity of DNA-Arc interaction. *Protein Sci* **1993,** *2*, 945-950.
28. Arakawa, T.; Timasheff, S. N. The mechanism of action of Na glutamate, lysine HCl, and piperazine-N, N'-bis (2-ethanesulfonic acid) in the stabilization of tubulin and microtubule formation. *J. Biol. Chem.* **1984,** *259*, 4979-4986.
29. Auton, M.; Bolen, D. W.; Rosgen, J. Structural thermodynamics of protein preferential solvation: Osmolyte solvation of proteins, aminoacids, and peptides. *Proteins* **2008,** *73*, 802-813.
30. Canchi, D. R.; Garcia, A. E. Cosolvent effects on protein stability. *Annu Rev Phys Chem* **2013,** *64*, 273-293.
31. Capp, M. W.; Pegram, L. M.; Saecker, R. M.; Kratz, M.; Riccardi, D.; Wendorff, T.; Cannon, J. G.; Record, M. T. Interactions of the Osmolyte Glycine Betaine with Molecular Surfaces in Water: Thermodynamics, Structural Interpretation, and Prediction of m-Values. *Biochemistry* **2009,** *48*, 10372-10379.
32. Guinn, E. J.; Pegram, L. M.; Capp, M. W.; Pollock, M. N.; Record, M. T. Quantifying why urea is a protein denaturant, whereas glycine betaine is a protein stabilizer. *P Natl Acad Sci USA* **2011,** *108*, 16932-16937.
33. Rosgen, J.; Pettitt, B. M.; Bolen, D. W. An analysis of the molecular origin of osmolyte-dependent protein stability. *Protein Sci* **2007,** *16*, 733-743.
34. Santoro, M. M.; Liu, Y.; Khan, S. M.; Hou, L. X.; Bolen, D. W. Increased thermal stability of proteins in the presence of naturally occurring osmolytes. *Biochemistry* **1992,** *31*, 5278-5283.
35. Timasheff, S. N. The control of protein stability and association by weak interactions with water: How do solvents affect these processes? *Annu. Rev. Biophys. Biomol. Struct.* **1993,** *22*, 67-97.

36. Papini, C. M.; Pandharipande, P. P.; Royer, C. A.; Makhatadze, G. I. Putting the Piezolyte Hypothesis under Pressure. *Biophys J* **2017,** *113*, 974-977.
37. Merrin, J.; Kumar, P.; Libchaber, A. Effects of pressure and temperature on the binding of RecA protein to single-stranded DNA. *Proceedings of the National Academy of Sciences* **2011,** *108*, 19913.
38. Phadtare, S.; Inouye, M. Sequence-selective interactions with RNA by CspB, CspC and CspE, members of the CspA family of Escherichia coli. *Molecular microbiology* **1999,** *33*, 1004-1014.
39. Bae, W.; Xia, B.; Inouye, M.; Severinov, K. Escherichia coli CspA-family RNA chaperones are transcription antiterminators. *Proceedings of the National Academy of Sciences* **2000,** *97*, 7784.
40. Feng, Y.; Huang, H.; Liao, J.; Cohen, S. N. Escherichia coli poly(A)-binding proteins that interact with components of degradosomes or impede RNA decay mediated by polynucleotide phosphorylase and RNase E. *The Journal of biological chemistry* **2001,** *276*, 31651-31656.
41. Vezzi, A.; Campanaro, S.; D'Angelo, M.; Simonato, F.; Vitulo, N.; Lauro, F. M.; Cestaro, A.; Malacrida, G.; Simionati, B.; Cannata, N.; Romualdi, C.; Bartlett, D. H.; Valle, G. Life at depth: Photobacterium profundum genome sequence and expression analysis. *Science (New York, N.Y.)* **2005,** *307*, 1459-1461.

For Table of Contents Use Only